J Electr Eng Technol.2015;10(1): 429-435
http://dx.doi.org/10.5370/JEET.2015.10.1.429

ISSN(Print) 1975-0102
ISSN(Online) 2093-7423

A Design of Prototype 1C2M Railway Vehicle Propulsion Control System Considering Slip Reduction of Traction Motor

Chin-Young Chang*, Jae-Moon Kim and Yoon-Ho Kim†**

Abstract – This study proposes a re-adhesion algorithm that has stable traction effort for rolling stock slip/slide minimization when deliverable traction decreases by slip. The proposed scheme estimates appropriate reference speed using two encoders for reducing slip and controls traction effort stably and has stable control characteristics for disturbance. The algorithm which uses the maximum adhesive effort by instantaneous estimation of adhesion force stably controls traction effort and gives rolling stock excellent acceleration and deceleration characteristics. And a slip sensing element that can quickly detect slip is used. Load motor and inverter were checked in various slip conditions for creating various line conditions.

Keywords: Railway vehicle, Propulsion control system, Adhesion effort, Slip

1. Introduction

Recently, to increase transportation capacity of railway vehicles, a method to reduce transportation time by upgradeing accelerating/decelerating capacity, and running speed is used. Railway vehicle drives wheels by applying induction motor as traction motor using propulsion control system. Thus, an important element to upgrade its performance to increase the speed is to make it lighter.

However, since railway vehicle creates tractive force with friction between vehicle wheel and rail, the decrease of adhesion by decreased vehicle weight can cause slip and slide when driving force is over adhesion. When slip occurs, adhesion between vehicle wheel and rail decreases, reducing tractive force remarkably, and causing mechanical damage and noises. Thus, it is necessary to apply re-adhesion control, and enhance tractive force, and reduce friction of wheel and rail. Therefore, in upgrading accelerating / decelerating capacity, making the vehicle run faster, it is necessary to have a method to control slip rapidly, and to use the maximum adhesive effort which is the limiting value in changing abrasive force to tractive force as well as to upgrade propulsion control system.[1-2]

This paper is a study on propulsion control system of railway vehicle to reduce slip on traction motor. The new system can control tractive force more stably than existing re-adhesion control system, and it can also stably control system disturbance. It is a control method to prevent slip by comparing speed of the traction motor receiver from encoder, and, if slip occurs, changing reference speed of the control system under the slip detection value. In addition, it applies slip detector which quickly detects slip occurrence to re-adhesion control. To realize such a re-adhesion control algorithm, this study designed and built small-sized railway vehicle propulsion control system of 4.8[kW] lC2M. Re-adhesion performance of 1C2M control is low. But main circuit configuration is simple and economical. In addition, to experiment slip occurrence in various slip conditions, it identified stable movement of traction motor under various conditions of slip occurrence using inverter as load. To realize the suggested control algorithm in real time, it applied high-performance DSP TMS320F28335.

† Corresponding Author: Dept. of Electrical and Electronics Engineering, Chung-Ang University, Korea. (yhkim@cau.ac.kr)
* Dept. of Electrical and Electronics Engineering, Chung-Ang University, Korea. (ccy9247@hanmail.net)
** Dept. of Transportation System Engineering, Korea National University of Transportation, Korea. (goldmoon@ut.ac.kr)
Received: July 23, 2014; Accepted: September 24, 2014

2. Re-adhesion Control of Railway Vehicle

2.1 Slip of railway vehicle

The driving force generated by traction motor is delivered to the vehicle wheel through gear and axle, and the driving force delivered to the vehicle wheel is delivered to railway vehicle through friction force expressed by the multiplication of the coefficient of friction between wheel and rail and weight of the railway vehicle. In this case, tangential force generated by friction force works to the opposite direction, and, this force is called adhesive effort, which works as tractive force determining propulsive force.

Fig. 1 shows the relationship among wheel, rail, and adhesive effort. As shown in Eq. (1) adhesive effort F_{AE} is expressed by coefficient of adhesion μ_{AE} and vehicle weight $W \cdot g$. As shown in Eq. (2) the equation of motion of railway vehicle can be expressed by the relationship between weight on wheel axle M and speed of railway vehicle. ($R(v_t)$: resistance to vehicle running)

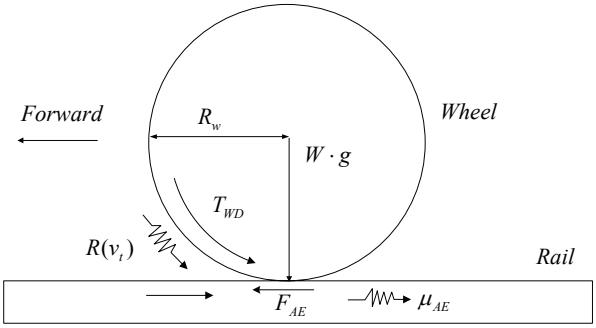

Fig. 1. Characteristics of Adhesive effort

$$F_{AE} = \mu_{AE} \cdot W \cdot g \tag{1}$$

$$M \cdot \frac{d}{dt} v_t = \mu_{AE} \cdot W \cdot g - R(v_t) \tag{2}$$

Motion characteristics of railway vehicle wheel is expressed by moment of inertia J and wheel speed ω_w, as shown in Eq. (3) (T: wheel driving torque, R_w: wheel radius).

$$J \cdot \frac{d}{dt} \omega_w = T - \mu_{AE} \cdot W \cdot g \cdot R_w \tag{3}$$

Equations for wheel and traction motor are expressed by (4), (5), and (6). If they are substituted in Eq. (3), they are expressed as Eq. (7) (v_w: wheel speed, M_j: weight on wheel, F_t: driving force of wheel).

$$v_w = \omega_w \cdot R_w \tag{4}$$

$$M_j = J / R_w^2 \tag{5}$$

$$F_t = T / R_w \tag{6}$$

$$M_j \cdot \frac{d}{dt} v_w = F_t - \mu_{AE} \cdot W \cdot g \tag{7}$$

Traction motor is expressed by Eqs. (8), (9), and (10). If they are substituted in Eq. (3), they are expressed as Eq. (11) (ω_w: motor rotation angular velocity, R_g: gear rate, T_m: motor torque, J_m: motor moment of inertia).[3-5]

$$\omega_m = \omega_w \cdot R_g \tag{8}$$

$$T = T_m \cdot R_g \tag{9}$$

$$J_m = \frac{J}{R_g^2} \tag{10}$$

$$J_m \cdot \frac{d}{dt} \omega_m = T_m - \frac{1}{R_g} \mu_{AE} \cdot W \cdot g \cdot R_w \tag{11}$$

Fig. 2 shows the block diagram of slip speed v_s estimated by Equations from (1) to (11). We can identify the elements by which we can estimate slip speed changes depending on motor torque T_m.

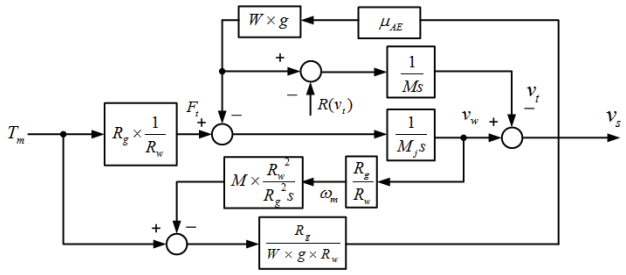

Fig. 2. Block diagram of slip speed estimation

2.2 Railway vehicle slip detection method

Railway vehicle slip can be detected as shown in Fig. 3. KTX - Sancheon detects with following (a) detection method by dividing vehicles into existing line and high-speed line, and comparing speed of four axles and vehicle speed transmitted by communications, and by setting detection reference speed v_{dm}.

(a) slip speed $v_s \geq$ detection reference value v_{dm}
(b) motor acceleration $\alpha_M \geq$ detection reference value α_{dm}
(c) slip acceleration $\alpha_S \geq$ detection reference value α'_{dm}

If slip speed is faster than detection reference value, it is possible to detect stably about changing environment. But rapid control is impossible because of slow detection. In the case of (a), though slip detection is stable, detection is slow. In the cases of (b) and (c), detection speed is faster than the case of (a). But, since they are sensitive to small changes of motor speed, being unstable to system disturbances, for complemental purposes, it is necessary to use low-pass filter component of acceleration speed as slip detection.

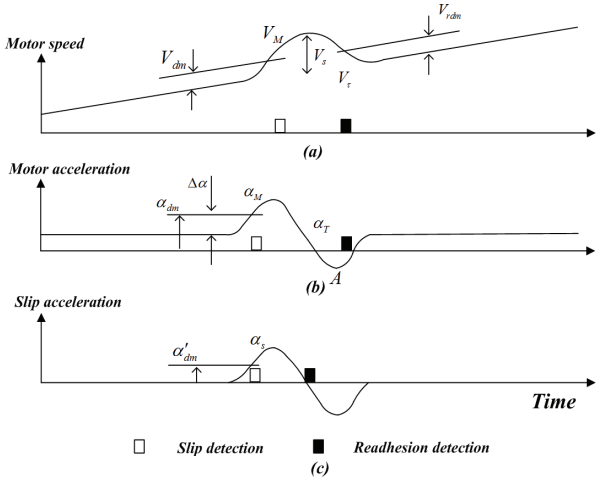

Fig. 3. Detection methods of Re-adhesion and slip

Table 1 is the slip detection method of KTX-Sancheon. It controls by dividing the time of driving and braking on the basis of the vehicle speed 150[km/h]. [6]

Table 1. Slip detection method (KTX-Sancheon)

	Low Speed Railway	High Speed Railway
Traction	- $v_s = v_w - v_t$ - $v_t \le 150[km/h]$ $v_s \ge v_{dm} : 5[km/h]$	- $v_s = v_w - v_t$ - $v_t > 150[km/h]$ $v_s \ge v_{dm} : 8[km/h]$
Brake	- $v_s = v_w - v_t$ - $v_t \le 150[km/h]$ $v_s \ge v_{dm} : 5[km/h]$	- $v_s = v_w - v_t$ - $v_t > 150[km/h]$ $v_s \ge v_{dm} : 8[km/h]$

2.3 Railway vehicle re-adhesion control method

If slip occurs, it is necessary to re-adhere vehicle wheel and rail. To do it, it is necessary to apply reduced control of driving force. If re-adhesion is realized, it is necessary to apply control of increased driving force.

There are two patterns in decrease and increase of re-adhesive effort as shown in Fig. 4: straight line pattern like (a), (b), (c), and exponential function pattern like (d), (e), (f). Though the straight line function pattern shows rapid re-adhesion, tractive force is reduced too much. And, though it shows rapid recovery of driving force, big re-slip happens when adhesion is reduced. Exponential function pattern shows rapid re-adhesion and recovery, and reduces loss of tractive force, and probability and size of re-slip. But, if friction reduction is big, driving force recovery control has steeper slope than straight line increase, causing bigger slip speed. Re-adhesion control of KTX-Sancheon is made with (b) pattern which measures speeds of four wheels at the same time, and acquires railway vehicle speed measured by signal detector of the control system. If slim is detected by such a method, re-adhesion control is performed as a pattern shown in Table 2. [6]

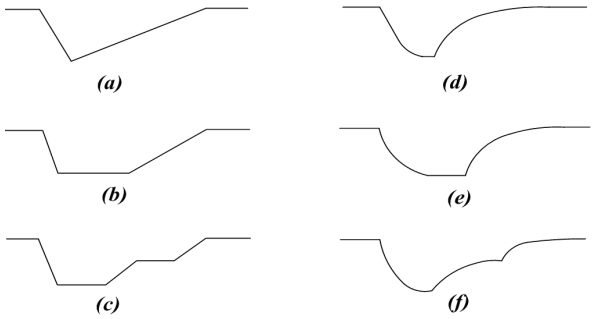

Fig. 4. Pattern of re-adhesive effort generation

Table 2. Re-adhesion control method (KTX-Sancheon)

	Low speed railway	High speed railway
Traction	- slip detection ⇒ powering 20[%] for 5[sec] - powering 60[%] for 5[sec]	- slip detection ⇒ powering 20[%] for 2[sec] - powering 100[%] for 10[sec]
Brake	- slip detection ⇒ braking 20[%] for 5[sec] - braking 60[%] for 5[sec]	- slip detection ⇒ braking 20[%] for 5[sec] - braking 100[%] for 10[sec]

2.4 Electric current-toque relation with respect to slip

Analysis shows that the elements affecting slip speed in Fig. 2. (Block diagram of slip speed estimation) are arithmetic operation of various parameters such as vehicle weight, gear rate, motor toque, coefficient of adhesion, and wheel radius, etc. Among these, coefficient of adhesion is affected by non-linear conditions such as rail moisture, dust, and oil, etc. Thus, when it is assumed that the vehicle operates with the maximum adhesive effort, vehicle radius seems to be an important element to calculate slip speed.

Fig. 5 is a graph measuring the difference of input current flowing from inverter to tractor motor following the change of operation speed of railway vehicle when the wheel diameter gap is 9[mm]. Let's call the traction motor connected with the axle whose wheel diameter is smaller as axle A, and that connected with the axle whose wheel diameter is larger as axle B. When the vehicle was running under 100 km/h, and its speed was reduced to 60 km/h, the current difference became large, about 80 km/h. On average, the gap was less than 20[A].

Table 3 shows comparison of different tractive forces caused by reference adhesive effort and differences in wheel diameter. When the wheel diameter gap is 12[mm], 200[km/h], and, when the gap is 9[mm], slip occurs after 250[km/h]. Consequently, the smaller the wheel diameter gap in the same vehicle, the less slip occurs in whole ranges.

In Table 4, when the wheel diameter gap is 12[mm], and

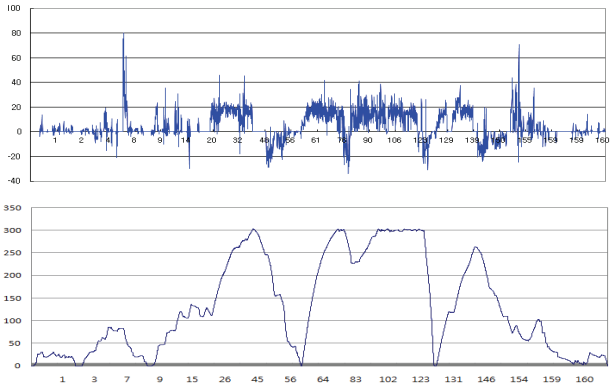

Axle x: distance[km], Axle y: current[A]

Fig. 5. Gap of input current of traction motor [9mm]

Table 3. Tractive force of traction motor

Speed [km/h]	Tractive force [kN]						Adhesive effort [kN]
	4mm		9mm		12mm		
	Axle A	Axle B	Axle A	Axle B	Axle A	Axle B	
0	25.62	26.61	24.51	30.10	22.94	31.55	51.09
50	25.62	26.61	24.51	30.10	22.94	31.55	48.96
100	25.66	26.91	21.21	32.89	19.31	35.61	46.84
150	23.17	24.37	16.38	27.35	15.11	31.20	39.60
200	23.25	24.70	15.29	30.59	11.67	35.93	32.36
250	22.45	23.99	14.76	30.17	11.54	33.91	27.70
300	22.15	23.56	14.80	29.07	11.00	33.13	23.03

Table 4. Phase current of traction motor

Speed [km/h]	Phase current [A] of traction motor depending on wheel diameter gap					
	4mm		9mm		12mm	
	Axle A	Axle B	Axle A	Axle B	Axle A	Axle B
0	351.41	364.88	336.09	412.84	314.64	432.62
50	351.41	364.88	336.09	412.84	314.64	432.62
100	351.86	369.04	290.83	451.04	264.76	488.41
150	317.82	334.15	224.59	375.10	207.16	427.93
200	318.92	338.64	209.64	416.46	160.00	492.81
250	307.91	329.06	202.41	410.05	158.26	465.01
300	303.81	323.10	202.97	398.61	150.91	454.38

when the motor phase current difference is maximum motor is 333[A] at speed of 200[km/h], which is the same as slip occurs. And, when the wheel diameter gap is 9[mm], the phase current difference of 208 [A] at the maximum appeared at the speed of 250 [km/h], which is the same point where slip occurred. Therefore, in order to reduce slip occurrence, it is necessary to minimize the current difference between axles of traction motor.

3. Simulation

Fig. 6 shows construction of simulation. To design a propulsion control system which can reduce slip of traction motor, we did various simulations using parameters of small type model of Table 5. To converter, PLL control and output voltage were applied, and to inverter, indirect vector control and instantaneous re-adhesion control to reduce slip were applied.

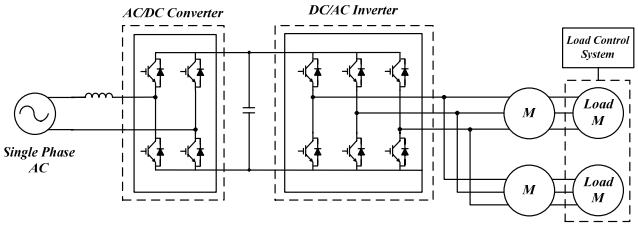

Fig. 6. Construction of system

Table 5. Small type model parameters

Item	Parameter value	
Input voltage	AC 220[V], 60[Hz]	
Converter input current	25[A]	
System capacity	4.8[kW]	
Converter/Inverter output voltage	380[V]	220[V]
Converter/Inverter output current	15[A]	11[A]

3.1 Converter

Fig. 7 shows a 2-phase voltage generator made with the filter method. PLL method which is easy to realize and has good performance was used.

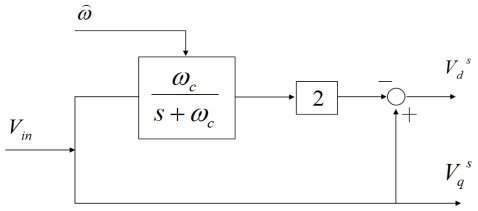

Fig. 7. Block diagram of 2 phase voltage generator

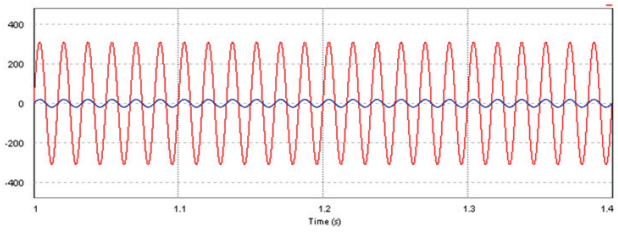

Axle x: div. 0.1[sec], Axle y: div. 200[V], div. 200[A]

Fig. 8. Converter voltage and current waveform

The block diagram shows that it gets phase and frequency by receiving catenary single phase alternating voltage V_{in}, and generating catenary voltage, and signal of phase difference $\pi/2$.

Fig. 8 shows converter input voltage and current wave form. We can identify that voltage and current are the same phase, and their power factor is 1.[7]

3.2 Inverter

Inverter switching was done by SVPWM control, and speed control of induction motor was done by indirect vector control. Simulation was done by realizing driving mode where standard speed was raised from 0 to 200[rpm], from 0.5[s] to 500[rpm], and from 1[s] to 1,000[rpm], and its characteristics was confirmed. [8-11]

Fig. 9 shows the diagram of real speed following the changes of reference speed (0⇒200⇒500⇒1,000[rpm]). We can identify that rotating speed of motor follows exactly the changes of reference speed.

Fig. 10 shows re-adhesion control output waveform by patterns. As shown in (a), with real speed following the changes of reference speed, if slip is detected, reference speed is reduced by 20[%] for 2[sec], and, then, reference

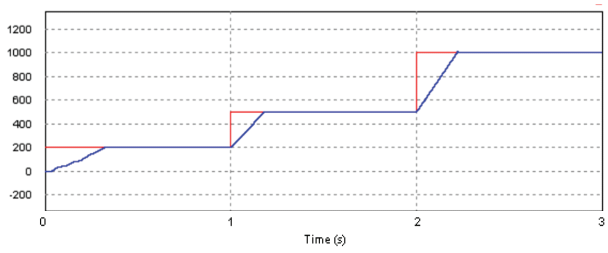

Axle x: div. 1[sec], Axle y: div. 200[rpm]

Fig. 9. Diagram of real speed following the changes of standard speed

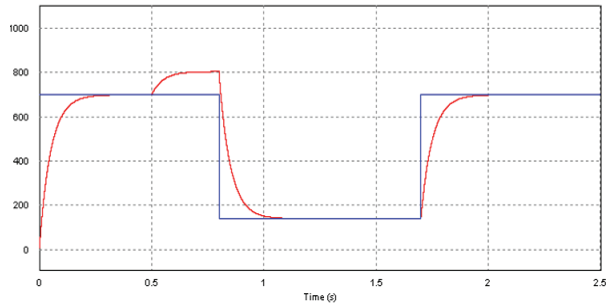

Axle x: div. 0.5[sec], Axle y: div. 200[rpm]

(a) Real speed and reference speed (pattern control)

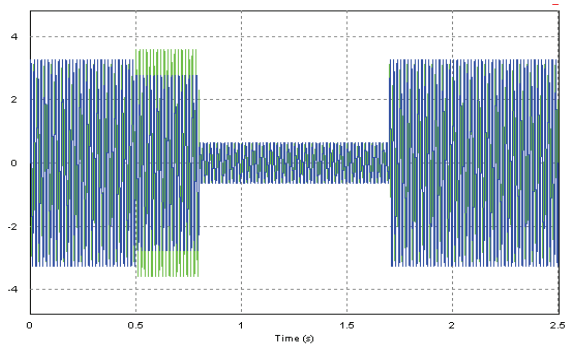

Axle x: div. 0.5[sec], Axle y: div. 2[A]

(b) Phase current of traction motor (pattern control)

Fig. 10. Re-adhesion control output waveform by patterns

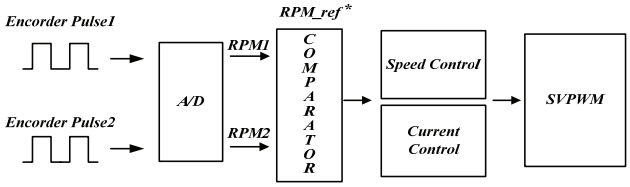

Fig. 11. Instantaneous re-adhesion control block diagram

speed is raised by 100[%]. Phase current waveform (b) of traction motor shows that when slip is detected, current gap in each axle becomes larger.

Fig. 11 shows instantaneous re-adhesion control block diagram of inverter. We can estimate slip through speed information measured by each traction motor. When slip is detected by comparing the number of rotation per minute, new standard speed is determined by reflecting differences of traction motor speed calculated by comparator to control simultaneously the rotating speed of traction motors which made slip and normally operating traction motor.

Fig. 12 shows instantaneous re-adhesion control output waveform. As shown in (a), if slip is detected while real speed follows the changes of reference speed, reference speed is reduced by 80[%] for 0.3[sec], and it is controlled by new reference speed estimated to reduce current gap of axles. When we see phase current waveform (b) of traction motor, we can identify that current gap of axles is reduced by instantaneous re-adhesion control.

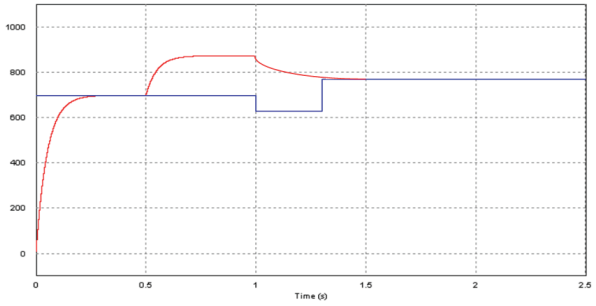

Axle x: div. 0.5[sec], Axle y: div. 200[rpm]

(a) Real speed and reference speed (proposed)

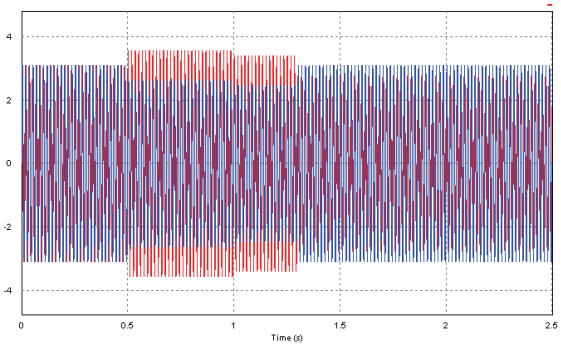

Axle x: div. 0.5[sec], Axle y: div. 2[A]

(b) Phase current of traction motor (proposed)

Fig. 12. Instantaneous re-adhesion control output waveform

4. Experiment

Fig. 13 shows experimental setup for railway vehicle propulsion control. To separate it from system power, it consists of double winding transformer, AC/DC converter, DC/AC inverter, two traction motors, and two loaded motors to generate slip. For converter and inverter, IGBT was applied, and they contain gate drive circuit and protective circuit. Main controller controls DSP, and sends gate signal to gate drive circuit with switching frequency of 10[kHz].

Fig. 14 shows propulsion control system output waveform. We can identify that (a) is controlled by converter output DC 380[V], and in the case of (b), current and current

Fig. 13. Experimental setup for railway vehicle propulsion control

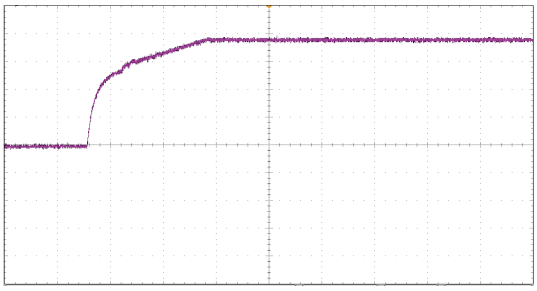

Axle x: div. 1[sec], Axle y: div. 100[V]

(a) DC-Link voltage

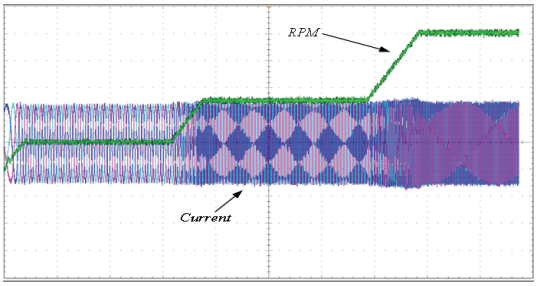

Axle x: div. 1[sec], Axle y: div. 200[rpm], div. 2[A]

(b) Real speed and Phase current

Fig. 14. Propulsion control system output waveform

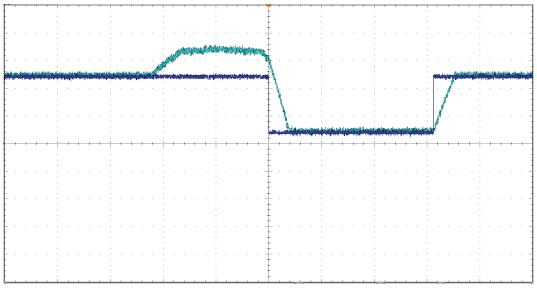

Axle x: Div. 1[sec], Axle y: Div. 300[rpm]

(a) Real speed according to reference speed (pattern control)

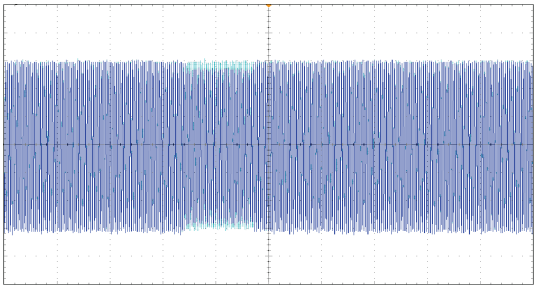

Axle x: div. 1[sec], Axle y: div. 200[rpm], div. 2[A]

(b) Phase current of traction motor (pattern control)

Fig. 15. Re-adhesion control output waveform by pattern

frequency rise depending on the changes of standard speed of traction motors. In simulation, while the current changes depending on changes in standard speed were big, we could identify changes of current frequency because of low load amount. But, the changes of current were small.

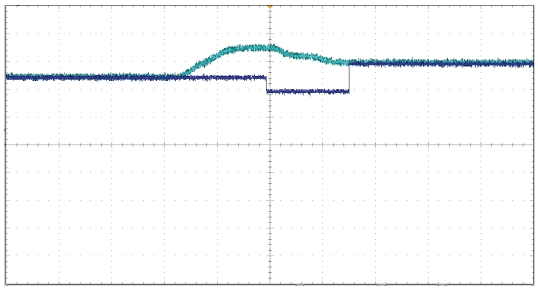

Axle x: Div. 1[sec], Axle y: Div. 300[rpm]

(a) Real speed according to reference speed (proposed)

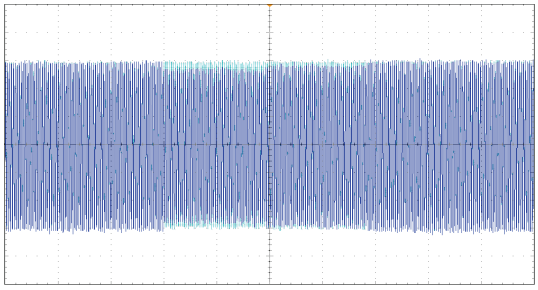

Axle x: Div. 1[sec], Axle y: Div. 2[A]

(b) Phase current of traction motor (proposed)

Fig. 16. Instantaneous re-adhesion control output waveform

Fig. 15 is re-adhesion control output waveform where speed gap between two motors is over 100[rpm] over 2[sec]. When they run, it detects as slip and perform re-adhesion control.

As shown in (a), while speed increases following the changes of reference speed, reference speed is reduced by 20[%] for 3[sec], and reference speed is raised by 100[%]. In the phase current waveform (b) reveals that when slip is detected in axles, the current gap of axles is smaller than the case of simulation, which is small change of current change by low load.

Fig. 16 shows instantaneous re-adhesion control output waveform. As shown in (a), if slip is detected, tractive force is reduced by 80[%] for 0.5[sec]. Then, it controls by estimating new reference speed. Thus, the time to return to reference speed is quick. In addition, phase current waveform (b) of traction motors reveals that it is more useful than re-adhesion control by pattern, in the efficient inverter.

5. Conclusion

To reduce slip which occurs when traction motor runs, this paper analyzed pattern re-adhesion control method and suggested instantaneous re-adhesion control algorithm by modeling 1C2M railway vehicle propulsion control system through PSIM S/W. In addition, we did the experiment by manufacturing scaled-down 4.8[kW] traction motor

propulsion control system, and slip occurrence simulation. The analysis of its characteristics led to the following conclusions.

1) Among elements affecting slip occurrence of railway vehicle, wheel radius is important to calculate slip speed. The difference of wheel radius causes current difference flowing in each axle, causing slip to occur.
2) Railway vehicle propulsion control system measures current difference which affects slip occurrence by encoder in real time, and estimate new tractive force and run.
3) The converter is built to control power factor as 1 by PLL control using hypothetical 2-phase method. It traction motor speed is controlled by the inverter system having induction motor with indirect vector control method.
4) The comparative analysis of re-adhesion control method by pattern and suggested instantaneous re-adhesion control method revealed that, when slip occurs, the latter is faster than the former in returning to reference speed.

References

[1] S. Senini, F. Flinders, W. Oghanna, “Dynamic Simulation of Wheel-rail Interaction for Locomative Traction studies”, AESM/IEEE Joint Railroad Conf. Rec., pp. 27-34, 1993.

[2] Yoshki Ishikawa, Atsuo Kawamura, “Maximum Adhesive force Control in Super High-Speed Train" PCC-Nagaoka'97, pp. 951-954, 1997.

[3] T. Watanabe, M. Ogasa, S Ohe, “Improvement of Readhesive Characteristics of Electric Motor Vehicles”, STECH Conf. Rec., Vol. 2, pp.243-247, 1993.

[4] Kee-Young Jeon, Jeong-min Jho, Seung-Hwan Lee, Bong-Hwan Oh, Hun-gu Lee, Yong-joo Kim, Kyung-hee Han, “Anti-Slip Control by Adhesion Effort Estimation of 1C-4 Minimized Railway Vehicle using Load Torque Disturbance Observer”, KIPE, No. 4, Vol. 8, pp. 366-375, 2003.

[5] Gil-Dong Kim, Ho-Yong Lee, Tae-Ki Ahn, Jai-Sung Hong, Suk-Youn Han, Kee-Young Jeon, “Anti-Slip Control by Adhesion Effort Estimation of Railway Vehicle”, KSR, No. 4, Vol. 6, pp. 116-123, 2003.

[6] Jae-Moon Kim, “Slip/Slide Improvement Report”, Korea National Railroad College, 2011.

[7] No-Geon Jung, Chin-Young Chang, Cha-Jung Yun, Jae-Moon Kim, “Response Characteristic Analysis using Modeling of Propulsion System for 8200 Electric Locomotive”, KIEE, No.11, Vol.62, pp.1640-1646, 2013.

[8] Hyun-Woo Sim, June-Seok Lee, Kyo-Beum Lee, “A Simple Strategy for Sensorless Speed Control for an IPMSM During Startup and Over Wide Speed Range”, KIEE, No.5, Vol.9, pp.1582-1591, 2014.

[9] Abdelfatah Nasri, Abdeldjabar Hazzab, Ismail Khalil Bousserhane, Samir Hadjeri, Pierre Sicard, “Fuzzy-Sliding Mode Speed Control for Two Wheels Electric Vehicle Drive”, KIEE, No.4, Vol.4, pp.499-509, 2009

[10] Saïd Drid, Abdesslam Makouf, Mohamed-Saïd Naït-Saïd, Mohamed Tadjine, “Highly Efficient Control of the Doubly Fed Induction Motor”, KIEE, No. 4, Vol. 2, pp.478-484, 2007.

[11] A. Boucheta, I. K. Bousserhane, A. Hazzab, P. Sicard, M. K. Fellah, “Speed Control of Linear Induction Motor using Sliding Mode Controller Considering the End Effects”, KIEE, No.1, Vol.7, pp.34-45, 2012.

Chin-Young Chang received the M.S degree in Electrical and Electonics Engineering from Chung-ang University, Korea, in 2010. He is currently working toward the Ph. D. degree at Chung-ang University. His research interests are power electronics, railway vehicle, electric drive systems and flexible ac transmission systems.

Jae-Moon Kim received the B.S., M.S. and Ph.D. degrees in electrical engineering from the Sungkyunkwan University, Korea, in 1994, 1996 and 2000, respectively. During 2004~2011, he had been with Korea National Railroad College as a Professor in the Department of Rolling Stocks Electric. Since 2012, he has been with Korea National University of Transportation, where he is currently a Professor in the Department of Transportation system and Railroad Electronics Electric Engineering. His research interests are power electronics, traction motor drives, and their control systems. He is a member of the Korean Society for Railway and the Korean Institute of Electric Engineers.

Yoon-Ho Kim received the B.S. degree from Seoul National University, Korea, the M.S. degree from the State University of New York at Buffalo, and the Ph. D. degree from Texas A&M University, College Station, all in electrical engineering. Since 1987, he has been with Chung-ang University, Korea, is now a Professor in electrical engineering. His main interests are industrial electronics and drives. He has served as a President of the Korean Institute of Power Electronics and the Korean Society for Railway.